Scientific Research Publishing

Journal of Modern Physics, 2023, 14, 526-533
https://www.scirp.org/journal/jmp
ISSN Online: 2153-120X
ISSN Print: 2153-1196

Design of Four-Channel Demultiplexer Based on Whispering-Gallery Mode Resonators

Ximeng Feng, Jinsong Huang*, Hongwu Huang

School of Information Engineering, Jiangxi University of Science and Technology, Ganzhou, China
Email: *jshuangjs@126.com

How to cite this paper: Feng, X.M., Huang, J.S. and Huang, H.W. (2023) Design of Four-Channel Demultiplexer Based on Whispering-Gallery Mode Resonators. *Journal of Modern Physics*, **14**, 526-533.
https://doi.org/10.4236/jmp.2023.144029

Received: February 20, 2023
Accepted: March 21, 2023
Published: March 24, 2023

Abstract

A new four-channel demultiplexer of single photons is proposed, in which four microresonators are utilized to link the four drop waveguides and the bus waveguide. By adjusting the system parameters, the crosstalk effect of the multiple channel frequencies is suppressed, and multiple peak frequencies with high drop efficiencies in these output ports are achieved. As the 2 × 2 model is scalable, the proposed structure can provide potential applications in designing scalable optical devices.

Keywords

Optical Filtering, Scattering Theory, Optical Waveguide, Microresonator

1. Introduction

Optical drop filters are the important components in optical communication systems, as they have been employed as demultiplexers, routers, switches, etc. During the last decade, numerous researches on optical filtering has been performed in various systems, such as Bragg grating systems [1]-[6], photonic crystal structures [7]-[15], plasmonic systems [16] [17], and waveguide coupled microresonator systems [18] [19] [20] [21] [22], and so on. Specifically, whispering-gallery mode resonators as filter elements have drawn much concern due to their microscale sizes and ultra-high quality factors [23]. Using such a filter with very-low loss, the expected frequency with very-high drop efficiency can be transferred and selected from the bus waveguide to the drop waveguide.

As a scalable application of single channel filters, multi-channel filtering [24] [25] [26] [27] [28] has aroused wide attention, because the demultiplexer with multiple user ports can be used to implement multiplexing communication. However, the quality of transmission signals will be damaged by the crosstalk effect of

these signals, and thus it is of considerable interest to design a multi-channel demultiplexer with high drop efficiency and low crosstalk for a communication network.

Motivated by the above considerations, we propose a four-channel demultiplexer in which four drop waveguides are connected to a bus waveguide via intermediate coupled microresonators. By using the real-space approach, the scattering amplitudes of single photons in these output ports of drop waveguides are derived. Numerical results show that the crosstalk of the multiple central frequencies can be suppressed by increasing the inter-resonator detuning, and multiple peak frequencies with high drop efficiencies in these channels are realized by controlling the waveguide-resonator couplings. In contrast to the common schemes [7] [8] [9] requiring a reflector to reflow the forward photons and get more high drop efficiencies, the proposed structure needs no reflection feedbacks, due to the mode-direction matching between the photon and resonator modes. Moreover, the resonators are independent on their exact locations, which is helpful to save the placement spaces. The proposed compact demultiplexer as a module is easy to be extended to scalable devices, and therefore it can be applied in wavelength division multiplexing systems.

2. Theoretical Model

As displayed shown in **Figure 1**, a four-channel demultiplexer of single photons is constructed by a bus waveguide and four drop waveguides, and these waveguides are linked by four single-mode whispering-gallery resonators. These resonators are described by the creation operator $e_n^\dagger$ ($n=1,2,3,4$), with the resonance frequency ω_n. The coupling strength between four resonators and the bus waveguide is denoted as V_{an}. Similarly, V_{bn} describes the coupling strength between these resonators and these drop waveguides, respectively. When a single photon is incident from the left port of the bus waveguide, it is coupled to these resonators, and then dropped to these drop waveguides.

The total Hamiltonian via the real space approach [29] for the filtering system can be given by ($\hbar=1$)

$$\begin{aligned} H = & \sum_{n=1,2,3,4}\int \mathrm{d}x\left[-i\upsilon_g C_R^\dagger(x)\frac{\partial}{\partial x}C_R(x)+i\upsilon_g C_{Ln}^\dagger(x)\frac{\partial}{\partial x}C_{Ln}(x)\right] \\ & +\sum_{n=1,2,3,4}(\omega_n-i\gamma_n)e_n^\dagger e_n+\sum_{n=1,2}V_{an}\int \mathrm{d}x\delta(x)\left[C_R^\dagger(x)e_n+C_R(x)e_n^\dagger\right] \\ & +\sum_{m=3,4}V_{am}\int \mathrm{d}x\delta(x-d)\left[C_R^\dagger(x)e_m+C_R(x)e_m^\dagger\right] \\ & +\sum_{n=1,2}V_{bn}\int \mathrm{d}x\delta(x)\left[C_{Ln}^\dagger(x)e_n+C_{Ln}(x)e_n^\dagger\right] \\ & +\sum_{m=3,4}V_{bm}\int \mathrm{d}x\delta(x-d)\left[C_{Lm}^\dagger(x)e_m+C_{Lm}(x)e_m^\dagger\right]. \end{aligned} \tag{1}$$

Here, $C_R^\dagger(x)$ represents the generation of a right-moving photon at x in the bus waveguide, while $\left[C_{Ln}^\dagger(x)\right]$ represents the generation of a left-moving photon at x in the drop waveguide-n. υ_g denotes the group velocity of the

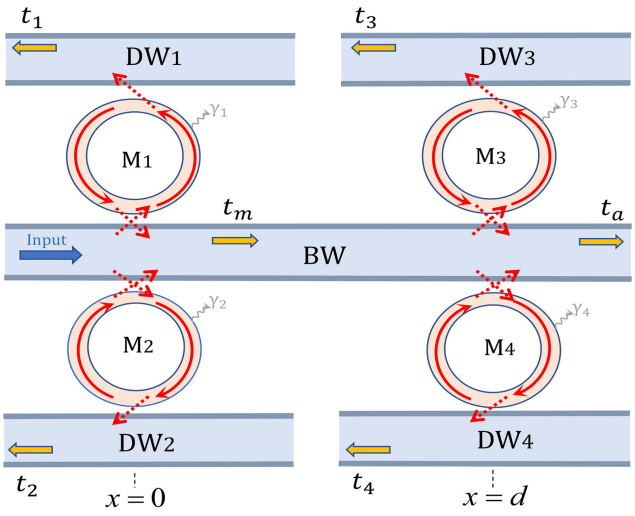

Figure 1. (Color online) Schematic view of a 2 × 2-shaped demultiplexer consisting of a bus waveguide (BW) and four drop waveguides (DWs), and four coupled single-mode whispering-gallery resonators. The input photon from the left side of the bus waveguide will be coupled to four microresonators (Mn), and transferred to four ports of these drop waveguides.

propagating photon. $\delta(x)\left[\delta(x-d)\right]$ means that the resonator-waveguide interaction occurs at $x=0(d)$. γ_n stands for the energy loss for these resonators.

The eigenstate of the Hamiltonian (1) is expressed as

$$|\psi\rangle=\int \mathrm{d}x\left[\phi_{R_a}C_{R_a}^{\dagger}+\phi_{L1}C_{L1}^{\dagger}+\phi_{L2}C_{L2}^{\dagger}+\phi_{L3}C_{L3}^{\dagger}+\phi_{L4}C_{L4}^{\dagger}\right]|\phi\rangle+\sum_{n=1,2,3,4}\xi_n e_n^{\dagger}|\phi\rangle, \quad (2)$$

$\phi_R(x)$ and $\phi_{Ln}(x)$ describe the single-photon wave functions along the right direction in the bus waveguide and the left direction in the drop waveguides, respectively. $|\phi\rangle$ describes the vacuum states of all waveguides and resonators. ξ_n represents the excitation amplitudes of these resonator modes.

The according wave functions can be described as

$$\begin{aligned}
\phi_{Ra} &= \mathrm{e}^{ikx}\left[\theta(-x)+t_m\theta(x)\theta(d-x)+t_a\theta(x-d)\right],\\
\phi_{L1} &= \mathrm{e}^{-ikx}t_1\theta(-x),\\
\phi_{L2} &= \mathrm{e}^{-ikx}t_2\theta(-x),\\
\phi_{L3} &= \mathrm{e}^{-ikx}t_3\theta(d-x),\\
\phi_{L4} &= \mathrm{e}^{-ikx}t_4\theta(d-x),
\end{aligned} \quad (3)$$

where, t_n represents the transmission amplitudes for four ports in these drop waveguides, and t_m and t_a represent the transmission amplitudes behind $x=0$ and $x=d$ in the bus waveguide, respectively. $\theta(x)$ denotes the Heaviside step function, with $\theta(0)=1/2$.

Suppose that a single photon is incoming from the left side of the bus waveguide with the energy $E_k=\omega$. By solving the eigen-equation $H|\psi\rangle=E_k|\psi\rangle$, these transmission amplitudes can be obtained as follows:

$$
\begin{aligned}
t_m &= 1-\frac{2iQ_2\Gamma_{a1}+2iQ_1\Gamma_{a2}+4\Gamma_{a1}\Gamma_{a2}}{Q_1Q_2+\Gamma_{a1}\Gamma_{a2}},\\
t_a &= t_m\left(1-\frac{2iQ_4\Gamma_{a3}+2iQ_3\Gamma_{a4}+4\Gamma_{a3}\Gamma_{a4}}{Q_3Q_4+\Gamma_{a3}\Gamma_{a4}}\right),\\
t_1 &= -\frac{2i\sqrt{\Gamma_{a1}\Gamma_{b1}}\left(Q_2-i\Gamma_{a2}\right)}{Q_1Q_2+\Gamma_{a1}\Gamma_{a2}},\\
t_2 &= -\frac{2i\sqrt{\Gamma_{a2}\Gamma_{b2}}\left(Q_1-i\Gamma_{a1}\right)}{Q_1Q_2+\Gamma_{a1}\Gamma_{a2}},\\
t_3 &= -\mathrm{e}^{2ikd}t_m\frac{2i\sqrt{\Gamma_{a3}\Gamma_{b3}}\left(Q_4-i\Gamma_{a4}\right)}{Q_3Q_4+\Gamma_{a3}\Gamma_{a4}},\\
t_4 &= -\mathrm{e}^{2ikd}t_m\frac{2i\sqrt{\Gamma_{a4}\Gamma_{b4}}\left(Q_3-i\Gamma_{a3}\right)}{Q_3Q_4+\Gamma_{a3}\Gamma_{a4}},
\end{aligned}
\tag{4}
$$

Here, $Q_n=\Delta\omega_n+i\gamma_n+i\Gamma_{an}+i\Gamma_{bn}$, $\Gamma_{an}=V_{an}^2/\left(2\upsilon_g\right)$, and $\Gamma_{bn}=V_{bn}^2/\left(2\upsilon_g\right)$. Generally, the transition frequencies of these resonators are different. Thus, we introduce these detunings as $\Delta\omega=\omega-\omega_{c1}$, which is the frequency detuning between the incident photon and the resonator-1, and $\Delta\omega_{1n}=\omega_1-\omega_n$, which is the frequency detuning between the resonator-1 and resonator-n. Then, $Q_n=\Delta\omega+\Delta\omega_{1n}+i\gamma_n+i\Gamma_{an}+i\Gamma_{bn}$ is rewritten for the sake of simplification.

3. Filtering Properties of Single Photons in the Coupled System

To characterize the filtering properties of the proposed system, we will investigate the transmission in the coupled system, which is denoted as $T_{a(1,2,3,4)}=\left|t_{a(1,2,3,4)}\right|^2$. As a contrast, we first consider the single-resonator case that only the drop waveguide-1 is coupled to the bus waveguide. When a single photon is incident from the left side of the bus waveguide, it will pass through the bus waveguide, or transmits to the left port of the drop waveguide-1 under the mode-direction matching condition between the resonator and waveguide modes.

Figure 2 displays the filtering spectra of single photons for different waveguide-resonator couplings when no dissipations are assumed. As shown from the green straight line, the total photon flow relation $T_a+T_1=1$ for two ports remains unchanged for any input frequencies. Moreover, a single drop peak for T_1 with maximal drop efficiency of 1 is represented at the resonance point $\Delta\omega=0$, for the equal waveguide-resonator couplings $\Gamma_{b1}=\Gamma_{a1}$. This means that the resonator behaves as a perfect mirror, and the moving photon along the bus waveguide is completely reflected on resonance, as investigated in Ref. [18]. To further examine the dependence of the drop efficiency on the couplings, the ratio $R=\Gamma_{b1}/\Gamma_{a1}$ is used to show their relationship in **Figure 2(d)**. It can be found that T_1 can get the maximum drop efficiency of unity only for $R=1$, arising from the fact that two same coupled routes between the resonators and waveguides are formed for two equal couplings, and thus the whole transfer over the two routes can be achieved.

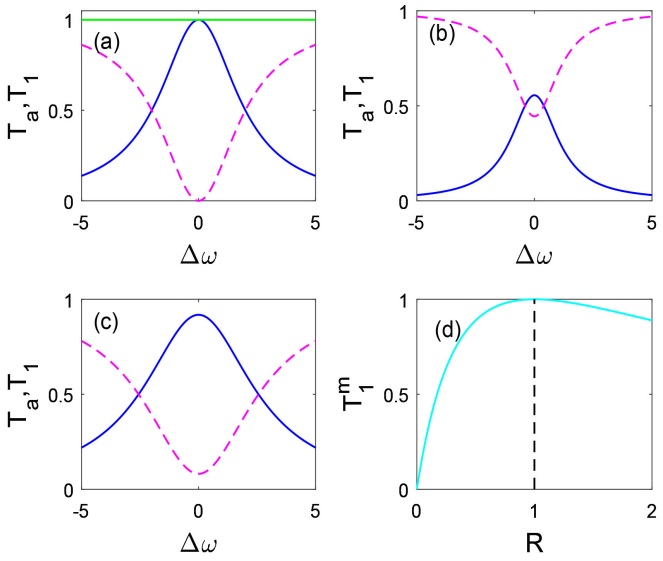

Figure 2. (Color online) The transmission T_a (pink dashed lines) and the drop efficiency T_1 (blue solid lines) for different coupling ratios: (a) $P=1$, (b) $P=0.2$, and (c) $P=1.8$. (d) The maximal drop efficiency T_1^m as a function of the coupling ratio *R*. Zero dissipation ($\gamma_1=0$) is assumed. For convenience, all the parameters are in units of Γ_{a1}.

When more waveguides are coupled to the bus waveguide through the coupled resonator, more transmission channels are generated. Consequently, the crosstalk emerges owing to the quantum interference from different transmission signals, which reduces the drop efficiencies of the filtering waves. The optical spectra in two output ports for the detuning $\Delta\omega$ are shown in **Figure 3(a)**, where two drop peaks with the central frequencies of $\Delta\omega_1$ and $\Delta\omega_2$ are presented. When tuning the inter-resonator detuning $\Delta\omega_{12}$ to broaden the resonance frequency interval, the crosstalk induced by quantum interference of two channel signals is reduced, and therefore the drop efficiencies of two channels are improved. Similarly, **Figure 3(b)** shows four drop peaks with unities for the appropriate detunings $\Delta\omega_{12}=\Delta\omega_{23}=\Delta\omega_{34}=20$, where the signal crosstalk from four channel signals can be suppressed by controlling the inter-resonator detunings. **Figure 3(c)** further displays the effect of the resonator-waveguide couplings on four drop peaks. For simplification, $R=\Gamma_{bn}/\Gamma_{an}$ is here taken as the coupling ratio and assumed to be same. As seen, four drop peaks in these channels emerge for four equal resonator-waveguide couplings, and a white straight line with $R=1$ passes through these crimson regions, since these symmetrical coupling paths among these waveguides results in the full transfers of these signals, as mentioned previously.

Note that these channel filterings are independent of the determined locations of these resonators, as indicated in Equation (4). In addition, compared with the previous schemes requiring the reflectors to reflow the forward photons to enhance the drop efficiencies [7] [8] [9], no reflection feedbacks are needed here due to the per-

fect transfers under the mode-direction matching condition. Thus, the 2×2 demultiplexer can scale up as a fixed module, for example, eight channel filtering $T_m\left(m=1,2,\cdots,8\right)$ with the drop efficiencies of unities are exhibited in **Figure 3(d)**, which has potential in wavelength division multiplexing communication.

Notice that the dissipations are not considered in the above investigations. In fact, the practical system inevitably suffers loss like the photon leakage from the waveguides and resonators. In contrast to the filtering spectra without dissipations, all of four drop efficiencies decrease with the increase of dissipations, as plotted in **Figure 4**. For a high-quality resonator with very low losses, however, high drop efficiencies are still obtainable, such as the desired result around 0.95 of T_n for $\gamma=0.05$. Here, equal dissipations $\gamma_n=\gamma$ are assumed.

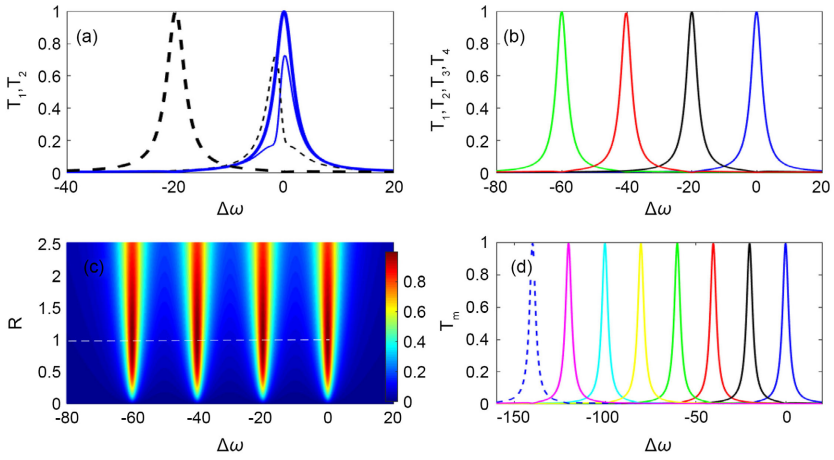

Figure 3. (Color online) (a) The drop transmission T_1 (blue solid lines) and T_2 (black dashed line) for different inter-resonator detunings: $\Delta\omega_{12}=1.5$ (thin lines) and $\Delta\omega_{12}=20$ (thick lines). (b) T_1, T_2, T_3, and T_4 (from the right to left) versus $\Delta\omega$. (c) T_1, T_2, T_3, and T_4 (from the right to left) as a function of $\Delta\omega$ and R. (d) Eight channel transmission T_m versus $\Delta\omega$. Other parameters are set as: $\Gamma_{bn}=\Gamma_{an}=1$, $\gamma_n=0$.

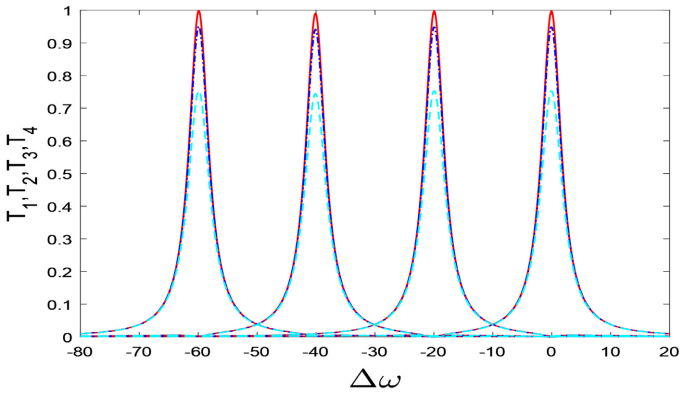

Figure 4. (Color online) T_1, T_2, T_3, and T_4 (from the right to left) for different dissipations: $\gamma=0, 0.05, 0.3$ (solid curves, dash dotted curves, dashed curves). Other parameters are the same as in **Figure 3**.

4. Conclusion

In summary, we have proposed a novel four-channel quantum demultiplexer of single photons in a coupled waveguide system. Our numeric results indicate that four drop peaks with high drop efficiencies within such a demultiplexer can be obtained in the scattering spectra, by tuning the inter-resonator frequency detunings and the resonator-waveguide couplings. In addition, as a fixed module, the compact demultiplexer is easy to scale up, which can be exploited in optical quantum communication.

Fund

This work was supported by Natural Science Foundation of Jiangxi Province (Grant No. 20212BAB201014).

Conflicts of Interest

The authors declare no conflicts of interest regarding the publication of this paper.

References

[1] Bilodeau, F., Johnson, D.C., Theriault S., Malo B., Albert, J. and Hill, K.O. (1995) *IEEE Photonics Technology Letters*, **7**, 388. https://doi.org/10.1109/68.376811

[2] Riziotis, C. and Zervas, M.N. (2001) *Journal of Lightwave Technology*, **19**, 92-104. https://doi.org/10.1109/50.914490

[3] Hamarsheh, M.M.N., Falah, A.A.S. and Mokhtar, M.R. (2015) *Optical Engineering*, **54**, Article ID: 016105. https://doi.org/10.1117/1.OE.54.1.016105

[4] Yun, B., Hu, G., Zhang, R. and Cui, Y. (2015) *Optics Communications*, **336**, 30-33. https://doi.org/10.1016/j.optcom.2014.09.048

[5] Zhang, Z.X., Mou, C.B., Yan, Z.J, Wang, Y.J., Zhou, K.M. and Zhang, L. (2015) *Optics Express*, **23**, 1353-1360. https://doi.org/10.1364/OE.23.001353

[6] Yang, J.J., Fan, J., Zou, Y.G., Wang, H.Z. and Ma, X.H. (2022) *Chinese Physics B*, **31**, Article ID: 084203. https://doi.org/10.1088/1674-1056/ac5391

[7] Kim, S., Park, I., Lim, H. and Kee, C.S. (2004) *Optics Express*, **12**, 5518. https://doi.org/10.1364/OPEX.12.005518

[8] Ren, H.L., Chun, J., Hu, W.S., Gao, M.Y. and Wang, J.Y. (2006) *Optics Express*, **14**, 2446. https://doi.org/10.1364/OE.14.002446

[9] Ren, H.L., Zhang, J.H., Qin, Y.L., Li, J., Guo, S.Q., Hu, W.S., Jiang, C. and Jin, Y.H. (2013) *Optik*, **124**, 1787-1791. https://doi.org/10.1016/j.ijleo.2012.05.017

[10] Qiang, Z.X., Zhou, W.D. and Soref, R.A. (2007) *Optics Express*, **15**, 1823-1831. https://doi.org/10.1364/OE.15.001823

[11] Monifi, F., Ghaffari, A., Djavid, M. and Abrishamian, M.S. (2003) *Applied Optics*, **48**, 804-809. https://doi.org/10.1364/AO.48.000804

[12] Barati, M. and Aghajamali, A. (2016) *Physica E*, **79**, 20-25. https://doi.org/10.1016/j.physe.2015.12.012

[13] Kumar, A., Suthar, B., Kumar, V., Bhargava, A., Singh, K.S. and Ojha, S.P. (2013) *Optik*, **124**, 2504-2506. https://doi.org/10.1016/j.ijleo.2012.08.030

[14] Wang, H.T., Timofeev, I.V., Chang, K., Zyryanov, V.Y. and Lee, W. (2014) *Optics*

Express, **22**, 15097. https://doi.org/10.1364/OE.22.015097

[15] Zhao, X.D., Yang, Y.B., Wen, J.H., Chen, Z.H., Zhang, M.D., Fei, H.M. and Hao, Y.Y. (2017) *Applied Optics*, **56**, 5463. https://doi.org/10.1364/AO.56.005463

[16] Khani, S., Danaie, M. and Rezaei, P. (2018) *Optical Engineering*, **57**, Article ID: 107102. https://doi.org/10.1117/1.OE.57.10.107102

[17] Geng, X.M., Wang, T.J., Yang, D.Q., He, L.Y. and Wang, C. (2016) *IEEE Photonics Journal*, **8**, Article ID: 4801908. https://doi.org/10.1109/JPHOT.2016.2573041

[18] Monifi, F., Friedlein, J., Özdemir, S.K. and Yang, L. (2012) *Journal of Lightwave Technology*, **30**, 3306. https://doi.org/10.1109/JLT.2012.2214026

[19] Monifi, F., Özdemir, S.K. and Yang, L. (2013) *Applied Physics Letters*, **103**, Article ID: 181103. https://doi.org/10.1063/1.4827637

[20] Zhou, Z.H., Chen, Y., Shen, Z., Zou, C.L., Guo, G.C. and Dong, C.H. (2018) *IEEE Photonics Journal*, **10**, Article ID: 7101607. https://doi.org/10.1109/JPHOT.2017.2764071

[21] Yin Y.H., Niu, Y.X., Dai, L.L. and Ding, M. (2018) *IEEE Photonics Journal*, **10**, Article ID: 7103810. https://doi.org/10.1109/JPHOT.2018.2849976

[22] Deng, L., Li, D.Z., Liu, Z.L., Meng, Y.H., Guo, X.N. and Tian, Y.H. (2017) *Chinese Physics B*, **26**, Article ID: 024209. https://doi.org/10.1088/1674-1056/26/2/024209

[23] Vahala, K.J. (2003) *Nature*, **424**, 839-846. https://doi.org/10.1038/nature01939

[24] Soma, S., Sonth, M.V. and Gowre, S.C. (2019) *Journal of Electronic Materials*, **48**, 7460-7464. https://doi.org/10.1007/s11664-019-07572-1

[25] Zhan, W.L., Xu, J.X., Zhao, X.L., Hu, B.J. and Zhang, X.Y. (2020) *IEEE Transactions on Circuits and Systems*, **67**, 2858-2862. https://doi.org/10.1109/TCSII.2020.2982409

[26] Zhou, K., Sun, X.X., Ma, H.Y. and Zhong, X.X. (2023) *IEEE Sensors Journal*, **23**, 3567-3572. https://doi.org/10.1109/JSEN.2023.3234544

[27] Huang, J.S. and Feng, X.M. (2023) *Journal of Modern Physics*, **14**, 101-110. https://doi.org/10.4236/jmp.2023.142007

[28] Huang, J.S. and Peng, H.Q. (2023) *International Journal of Theoretical Physics*, **62**, 42. https://doi.org/10.1007/s10773-023-05306-y

[29] Shen, J.T. and Fan, S.H. (2009) *Physical Review A*, **79**, Article ID: 023838. https://doi.org/10.1103/PhysRevA.79.039904